Bioinspired, Biomimetic and Nanobiomaterials

Tuning methods and mechanical modelling of hydrogels
Zhan and Niu

ice | science

http://dx.doi.org/10.1680/bbn.14.00029
Themed Issue Review Paper
Received 02/09/2014 Accepted 16/12/2014
Published online 20/12/2014
Keywords: biomaterial/material properties/modelling

ice Institution of Civil Engineers publishing

Tuning methods and mechanical modelling of hydrogels

1 **Yuexing Zhan** BS*
PhD Candidate, Department of Mechanical and Biomedical Engineering, City University of Hong Kong, Tat Chee Avenue, Kowloon, Hong Kong
Center for Advanced Structural Materials (CASM), City University of Hong Kong, Tat Chee Avenue, Kowloon, Hong Kong

2 **Xinrui Niu** PhD
Assistant Professor, Department of Mechanical and Biomedical Engineering, City University of Hong Kong, Tat Chee Avenue, Kowloon, Hong Kong
Center for Advanced Structural Materials (CASM), City University of Hong Kong, Tat Chee Avenue, Kowloon, Hong Kong

Hydrogels are cross-linked polymeric networks filled with high water content. They are used as tissue/cell culture scaffolds, biomedical devices and healthcare products. As the performance of hydrogels is significantly affected by their mechanical properties, it is required to tune hydrogels into desired mechanical systems. To provide guidance to the tuning process, it is important to evaluate and model the mechanical properties of hydrogels. However, due to the structural complexity of hydrogels, both tuning and modelling face challenges and uncertainties. This article briefly reviews the tuning methods and summarises key mechanical models that address linear elastic, hyperelastic, viscoelastic, poroelastic and hybrid mechanical behaviours of hydrogels.

1. Introduction

Hydrogels are widely used in healthcare industry and biomedical research.[1,2] The most popular usages include drug-delivery systems,[3–5] diapers,[6,7] contact lenses[8–10] and scaffolds for tissue engineering.[11–13] The mechanical properties of hydrogels play an important role in all these applications. Stiffness/toughness provides mechanical integrity and easiness to handle,[14,15] while softness allows flexibility, modulus matching with surrounding tissues and light weight.[16] Furthermore, for many applications, the mechanical properties of hydrogels have to be in a desirable range for the achievement of functions. For example, cells may only spread, differentiate and survive on the hydrogel scaffolds of certain stiffness.[17–22] To fulfill these demands, the mechanical properties of hydrogels need to be controlled. Not surprisingly, an in-depth understanding of the mechanical properties of hydrogels is required. This article summarises typical methods to tune the mechanical properties of hydrogels in the scope of mechanical engineering and reviews models that characterise the elastic mechanical properties of hydrogels.

2. Tuning methods

Since hydrogels are cross-linked polymeric networks (Figure 1(a)) with high water content,[23] it is natural to tune their mechanical properties by adjusting the network structures. The common methods include altering the cross-link density of the network, adding fillers, adjusting the hydrophobicity of hydrogels, modifying the structure of the pores and so on.

2.1 Altering the cross-link density

Obviously, cross-link density changes with the weight percentage and molecular weight of monomers. A common way to produce stiffer hydrogels is to select monomers that have a lower molecular weight or simply increase the weight percentage of monomers.[24,25] However, decreasing the molecular weight could significantly downgrade the ductility of hydrogels[26] while increasing the weight percentage of monomers obviously decrease the weight percentage of water content, which diminishes the benefits brought by the high water content such as nutrition supply to cells.

To fabricate the hydrogels with high modulus without sacrificing their ductility, double-networking (DN) method emerged out in the early twenty-first century.[27–32] As implied by its name, the DN hydrogel consists of two networks formed by different types of monomers (Figure 1(b)). At first, a densely cross-linked hydrogel network was fabricated with polymer A. Then, the A-type network

***Corresponding author e-mail address:** yxzhan4-c@my.cityu.edu.hk

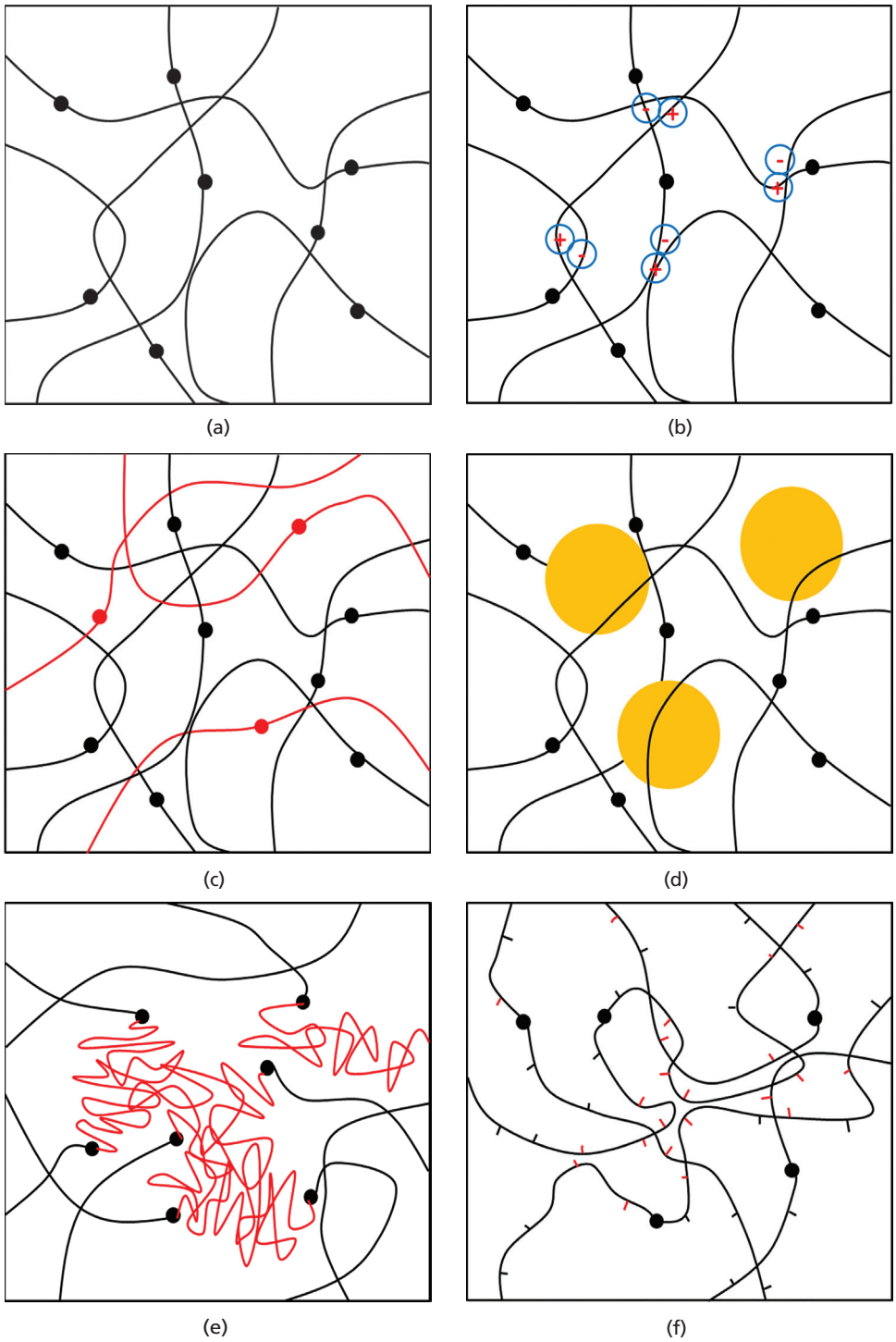

Figure 1. A schematic representation of a (a) hydrogel; (b) double-network (DN) hydrogel, where dots represent covalent bonds, red lines represent loosely cross-linked network, and black lines represent densely cross-linked network; (c) hydrogel with ionic bonds, where blue circles represent ionic bonds and black lines represent cross-linked network; (d) hydrogel reinforced with fillers (yellow circles); (e) hydrogel with hydrophobic monomers, where dots represent covalent bonds, black lines represent hydrophilic monomers and red lines represent hydrophobic monomers that tend to shrink and aggregate in water; (f) hydrogel synthesised by amphiphilic monomers, where black bars represent hydrophilic groups and red bars represent hydrophobic groups that tend to aggregate in water

was merged into the precursor of polymer B so a loosely cross-linked B-type network was formed and interpenetrated with the A-type network. Gong and co-workers[29] are the pioneers who produced the DN hydrogel. Compared to the individual networks, the DN hydrogel showed an optimised stiffness, a good ductility and a significantly enhanced failure stress[33] (Figure 2). Furthermore, they also suggested that the A-type network dominates the modulus enhancement while the B-type network maintains ductility, and the molar ratio between the two monomers could highly influence the properties of the DN hydrogel. In addition, compared to the conventional interpenetrating (IPN) hydrogel,[34–36] the DN hydrogel also shows better mechanical properties.[28] By optimising the combination of mechanical properties, the DN technique provides opportunities to fabricate hydrogels with patterned and gradient structures,[37–39] which will definitely benefit the research on cell differentiation and 3D scaffold construction. However, although the DN hydrogel is tough under monotonic loading, its fatigue properties are not satisfactory because the breakage of covalent bonds is not reversible.[32]

Another method to tune the mechanical properties of hydrogels by altering their cross-link density is to form more bonds between the monomers by introducing ionic bonds (Figure 1(c)). Henderson *et al*.[40] introduced ions, such as Zn^{2+} and Ca^{2+}, into a poly(methyl methacrylate)–poly(methacrylic acid)–poly(methyl methacrylate) (PMMA–PMAA–PMMA) hydrogel. By two disparate cross-linking mechanisms, the monomers were linked not only covalently (monomer–monomer) but also ionically (monomer–ion–monomer). From the results of uniaxial tensile tests,[40] it is clear that the stiffness of these hydrogels highly depends on the ion type, ion concentration and the pH value of the surrounding environment. For example, the modulus of the hydrogel with Zn^{2+} is higher than that of the hydrogel with Ca^{2+} at the same concentration. The modulus increases with an increase in the concentration of Ca^{2+} but increases dramatically at the beginning and decreases slightly afterwards with the increase in the concentration of Zn^{2+} at pH = 6. However, at pH = 4, the modulus exhibits a monotone increase for both Zn^{2+} and Ca^{2+}. Although there is just one single polymer network, the hydrogel with ionic bonds is cross-linked twice, just like the DN hydrogel.[32] However, the ionically cross-linked ones show a much better fatigue resistance since the ionic bonds are reversible[41] and even self-healable.[42]

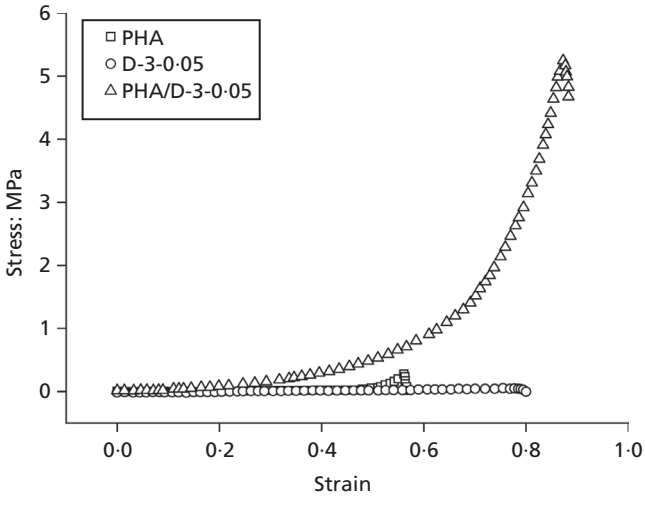

Figure 2. Stress–strain curves of PHA, D-3-0·05 and PHA/D-3-0·05 DN hydrogels obtained from uniaxial compression testsReprinted from Weng *et al*.[33]

2.2 Adding fillers

Numerous works have been performed to tune the mechanical properties of hydrogels by adding fillers (Figure 1(d)). The fillers could be ceramics such as silica and titania,[43–47] metals and their oxides such as silver and magnetic particles,[48–50] polymers,[51,52] carbon nanotubes and graphenes.[53–57] The size of the fillers varies from micrometre to nanometre scale.[24,43,55] Generally speaking, the higher the filler contents, the higher the mechanical properties were achieved[43,44,58] (Table 1). The smaller the filler size, the more efficient the enhancement on mechanical properties would be.[59–62] However, the experimental results also suggest that the mechanical properties, especially strength and toughness, could drop when the filler content is over a certain threshold,[63–65] which could be explained by the non-uniform distribution and aggregation of the fillers[43,63,64] (Figure 3), and weak bonds between the hydrogel network and fillers.[44,66] The dispersion status of the hydrogel/filler composites could be improved by magnetic stirring and ultrasonication methods. The bonds between the hydrogel network and fillers could be strengthened with particle surface treatment. These methods could significantly enhance the modulus and strength of the hydrogel/filler composites.[65,67]

To model and predict the influence of fillers on the mechanical properties of polymer/filler composites, many mathematical models were developed. Table 2 summarises several classical ones,[68–77] which are widely adopted on polymer composites. Although they were mostly applied to the composites with much stiffer matrix, the authors still list them here in the light of providing possibilities to gain a better understanding and prediction on the modulus of hydrogel/filler composites.

2.3 Adjusting the hydrophobicity

The stiffness of hydrogels increases with the enhancement of their hydrophobicity.[78] Hence, researchers added hydrophobic monomers into the highly hydrophilic network of hydrogels in the hope of promoting their stiffness. Cui *et al*.[79,80] formed such a hybrid hydrogel by linking poly(ethylene glycol) (PEG) monomer and poly(dimethylsiloxane) (PDMS) monomer with a cross-linker (Figure 1(e)). The hydrophobicity of the hydrogel was controlled by adjusting the weight percentage of PDMS monomer (Figure 4). The uniaxial compression tests (Figure 5) were then performed and

Hydrogels	Young's modulus: kPa	References
5% PEG + 0% silica NP	~3	43
5% PEG + 1% silica NP	~3	
5% PEG + 2·5% silica NP	~5	
5% PEG + 5% silica NP	~5	
5% PEG + 10% silica NP	~6	
6% PDMA + 0% silica NP	~25	58
6% PDMA + 1·5% silica NP	~50	
6% PDMA + 3·4% silica NP	~75	
6% PDMA + 5·4% silica NP	~115	
6% PDMA + 6·7% silica NP	~175	
6% PAAm + 0% silica NP	~25	44
6% PAAm + 1·5% silica NP	~28	
6% PAAm + 3·1% silica NP	~30	
6% PAAm + 5·1% silica NP	~35	
6% PAAm + 6·8% silica NP	~40	

Table 1. Young's moduli of hydrogels and hydrogel–silica nanocomposites. Data were obtained from uniaxial tensile tests

the experimental results demonstrated that the stiffness of the PEG/PDMS hybrid increased with the elevation of the hydrophobicity. Different from the Cui's approach, Liu *et al.*[81] synthesised amphiphilic monomers before gelation. The synthesised monomers had both hydrophobic and hydrophilic groups (Figure 1(f)). The stiffness of the hydrogel formed by this type of monomer could be tuned by controlling the degree of esterification (DE) of the hydrophobic and hydrophilic groups.[82] And the results indicated that the higher degree of DE led to higher stiffness.

In summary, high hydrophobicity could lead to high stiffness and high toughness, and it could enhance the therapeutic performance of hydrogels, such as increasing the encapsulation efficiency of a partially hydrophobic model drug.[81] But increasing the hydrophobicity will definitely decrease the water content, which may sacrifice the benefits of high water content.

2.4 Modifying the porous structures

It is also possible to tune the stiffness of hydrogels by modifying their porous structures since the pore size and density highly influence the mechanical properties of porous hydrogels.[83–85] One method to achieve porous structure is solvent casting/particle leaching, which is simple and could control the pore size by controlling pore-foaming agent size.[86] Delaney *et al.*[87] dispensed droplets of sodium alginate solution into a hardening bath of calcium chloride to form calcium alginate beads (pore-foaming agent) as shown in Figure 6(a). The beads were then added into other types of hydrogel precursor (solvent casting). After polymerisation, the beads were embedded into the hydrogel. When the hydrogel embedded with beads was washed by trisodium ethylene diamine tetraacetic acid solution, the calcium alginate beads dissolved (particle leaching) (Figure 6(b)) and eventually formed a macroporous matrix. Another method called polymer-phase separation[88] is similar to solvent casting/particle leaching. The pore-foaming agent is a removable phase. Tokuyama and Kanehara[89] added oil droplets (pore-foaming agent) into *N*-isopropylacrylamide (NIPA) hydrogel precursor. After polymerisation, the oil droplets were washed out by methanol and the porous NIPA hydrogel was obtained. In addition, frontal polymerisation is yet another method to fabricate porous hydrogels. Lu *et al.*[90] used sodium bicarbonate as a foaming agent to fabricate porous polyacrylamide hydrogel, and they also studied the effect of the concentration of foaming agent. In summary, these methods increase the pore size and density and produce soft but light hydrogels. Furthermore, the high surface-to-volume ratio and enlarged vacancy are in favour for the construction of a cell culture scaffold.[12]

3. Mechanical modelling

To tune hydrogels into the desired mechanical system, it is important to evaluate and model their mechanical properties.

3.1 Modulus

Although most hydrogels have non-linear stress–strain curves (Figure 2), modulus is still popular to quantify the elastic mechanical properties of hydrogels for its simplicity.[43,44,58,91] The modulus can be defined piece-wisely[43] or at a specific strain.[91,92] For the indentation-based experiments, Hertzian contact model is widely adopted to transform external loading into stress status. However, the Hertzian model is based on spherical or cylindrical indenters and does not consider the adhesive forces between the indenter and the hydrogel. Sneddon[93] provided a better alternative, especially for the indenters in shape of a paraboloid, cone or other sharp and axisymmetric geometries. Meanwhile, Derjaguin *et al.*[94] and Johnson *et al.*[95] addressed the adhesion behaviour by interpreting the adhesion acting outside or/and inside the contact region into additional terms of contact radius or/and indentation depth when dealing with the experimental data.[96] The models are well-known Derjaguin–Muller–Toporov (DMT) and Johnson–Kendall–Roberts (JKR) models.

3.2 Hyperelastic models

The hyperelasticity was first modelled in the 1940s by Ronald Rivlin[97] and Melvin Mooney[98] for non-linear elastic solids such as rubbers. A mechanistic Neo-Hookean model was developed by Rivlin, and a phenomenological Mooney–Rivlin model was proposed by Mooney in 1940 and expressed by Rivlin in 1948. In the late 60s and early 70s, Fung developed a 1D exponential

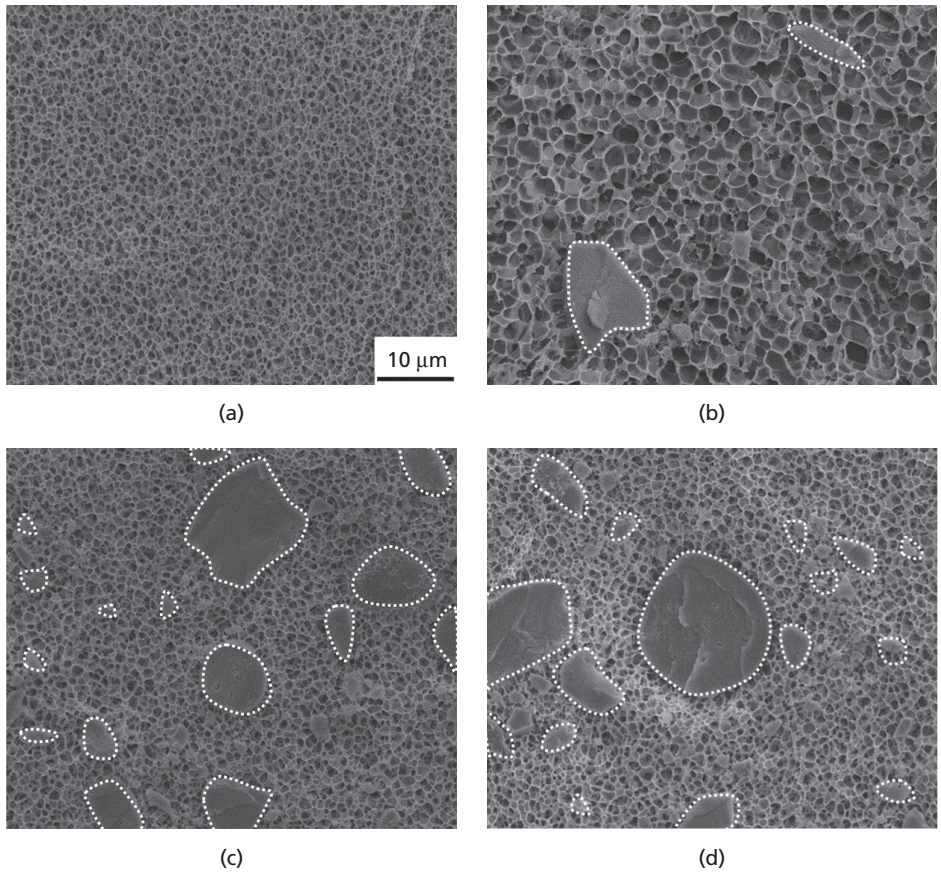

Figure 3. Cryo-SEM (scanning electron microscope) image of (a) PEG hydrogel and PEG–silica hydrogel nanocomposites with silica concentration of (b) 1%, (c) 5% and (d) 10%. The aggregations of silica nanoparticles were obvious at a higher silica concentrationReprinted from Gaharwar *et al*.[43]

Models	References
$E_c / E_m = 1 + 2 \cdot 5V_p$, where E_c and E_m represent the Young's moduli of the composite and the matrix, and V_p represents the volume fraction of the particle.	69,70
$E_c / E_m = 1 + 2 \cdot 5V_p + 14 \cdot 1V_p^2$	72
$E_c / E_m = \exp\left(\frac{2 \cdot 5V_p}{1 - sV_p}\right)$, where S is between 1 and 2.	74
$E_c / E_m = \frac{1 + A_1 B_1 V_p}{1 - \Psi B_1 V_p}$, $A_1 = k_E - 1$, $B_1 = \frac{E_p / E_m - 1}{E_p / E_m + A_1}$ and $\Psi = 1 + \left[\left(1 - V_{p_{max}}\right) / V_{p_{max}}^2\right] V_p$, where E_p represents the modulus of particle, k_E represents the Einstein's coefficient and $V_{p_{max}}$ represents the maximum packing fraction.	73,75,76
$\frac{1}{E_c} = \frac{1 - V_p^{1/2}}{E_m} + \frac{1}{\left(1 - V_p^{1/2}\right) / V_p^{1/2} E_m + E_p}$	68
$E_c = \chi_p E_p V_p + E_m\left(1 - V_p\right)$, where χ_p is between 0 and 1 or $\chi_p = 1 - \tanh\left(V_{p_{max}}\right) / V_{p_{max}}$.	71,77

Table 2. Models to predict the Young's modulus of composites

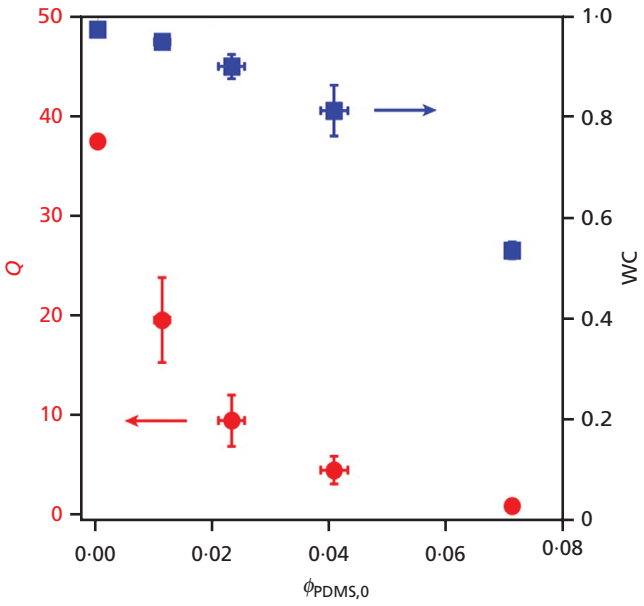

Figure 4. Swelling ratio (Q) and equilibrium water content (WC) against volume fraction of PDMSReprinted from Cui *et al.*[80]

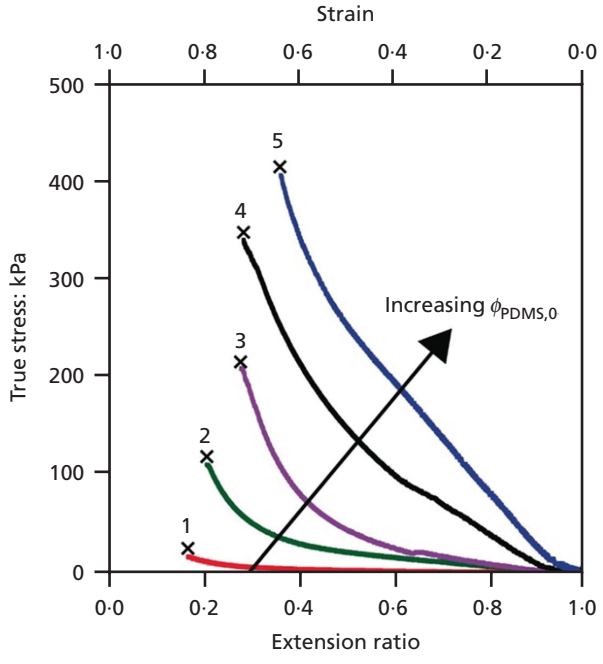

Figure 5. True stress–strain curves of hydrogels with increasing volume fraction of PDMSReprinted from Cui *et al.*[80]

constitutive equation for soft tissues,[99] while Ogden established a hyperelastic model, which could be reduced to the Neo-Hookean and Mooney–Rivlin models under certain material constants.[100] Other phenomenological models including the reduced polynomial Yeoh model[101] were also developed. The uniaxial forms of the above models are summarised in Table 3. Though widely adopted, except the Neo-Hookean model, they are all phenomenological, which means they may be able to fit the experimental data well but lack the capacity to explain the physical insights of polymer network structures and detailed physical processes involved in the deformation of hydrogels, nor predict the behaviour of the materials.

Mechanistically, the most significant advancement in the model development for hyperelastic materials was achieved by Arruda and Boyce[102] in 1993. Since the Arruda–Boyce model was derived by applying statistical mechanics to a cubic representative volume element (RVE), which contains eight chains connecting the centre with the vertexes, it is also called an eight-chain model. It is expressed in the following equation.

$$1. \qquad W = Nk_B\theta\sqrt{n}\left[\beta\lambda_{chain} - \sqrt{n}\ln\left(\frac{\sinh\beta}{\beta}\right)\right]$$

where N represents the number of chains in the network of a cross-linked polymer, k_B represents the Boltzmann constant, θ represents the temperature in Kelvin, n represents the number of chain segments, β represents the inverse Langevin function, $\beta = L^{-1}\left(\lambda_{chain}/\sqrt{n}\right)$, where the Langevin function is defined as $L(\beta) = \coth\beta - (\beta)$, and λ_{chain} represents the chain stretch, $\lambda_{chain} = \sqrt{I_1/3}$, where I_1 represents the first invariant of stretch.

Among all these hyperelastic models, in many cases, Ogden model could best fit the uniaxial experimental data as long as enough terms are used. Sasson and co-workers[103] evaluated the hyperelastic behaviour of chitosan hydrogel. The Moony–Rivlin, Neo-Hookean, Yeoh and Ogden models were all applied to fit the data. The five-term Ogden model provided the best fit for the experimental data. However, since there could be too many terms in the Ogden model, it is complicated mathematically and hard to be implemented into a computational framework. Hence, hyperelastic models other than the Ogden model are also widely adopted to describe the hyperelasticity of hydrogels. Faghihi *et al.*[104] evaluated the hyperelasticity of the graphene oxide/poly(acrylic acid)/gelation nanocomposite by fitting the uniaxial experimental data into the Neo-Hookean, Yeoh and Mooney–Rivlin models. The results indicated that the Yeoh model accurately defined the non-linear behaviour of this type of hydrogel. The Arruda–Boyce model was adopted by Zhao[105] to analyse the damage of the IPN hydrogel under large deformation. Under the framework constructed by the Arruda–Boyce model, Zhao quantitatively illustrated the basic mechanism of Mullins effect and necking instability in the IPN hydrogel. He also implanted it into the finite-element analysis, which showed a good agreement with the experimental data. However, due to the complexity of the Arruda–Boyce model, it is not as widely used in hydrogel modelling as the Ogden and Yeoh models.

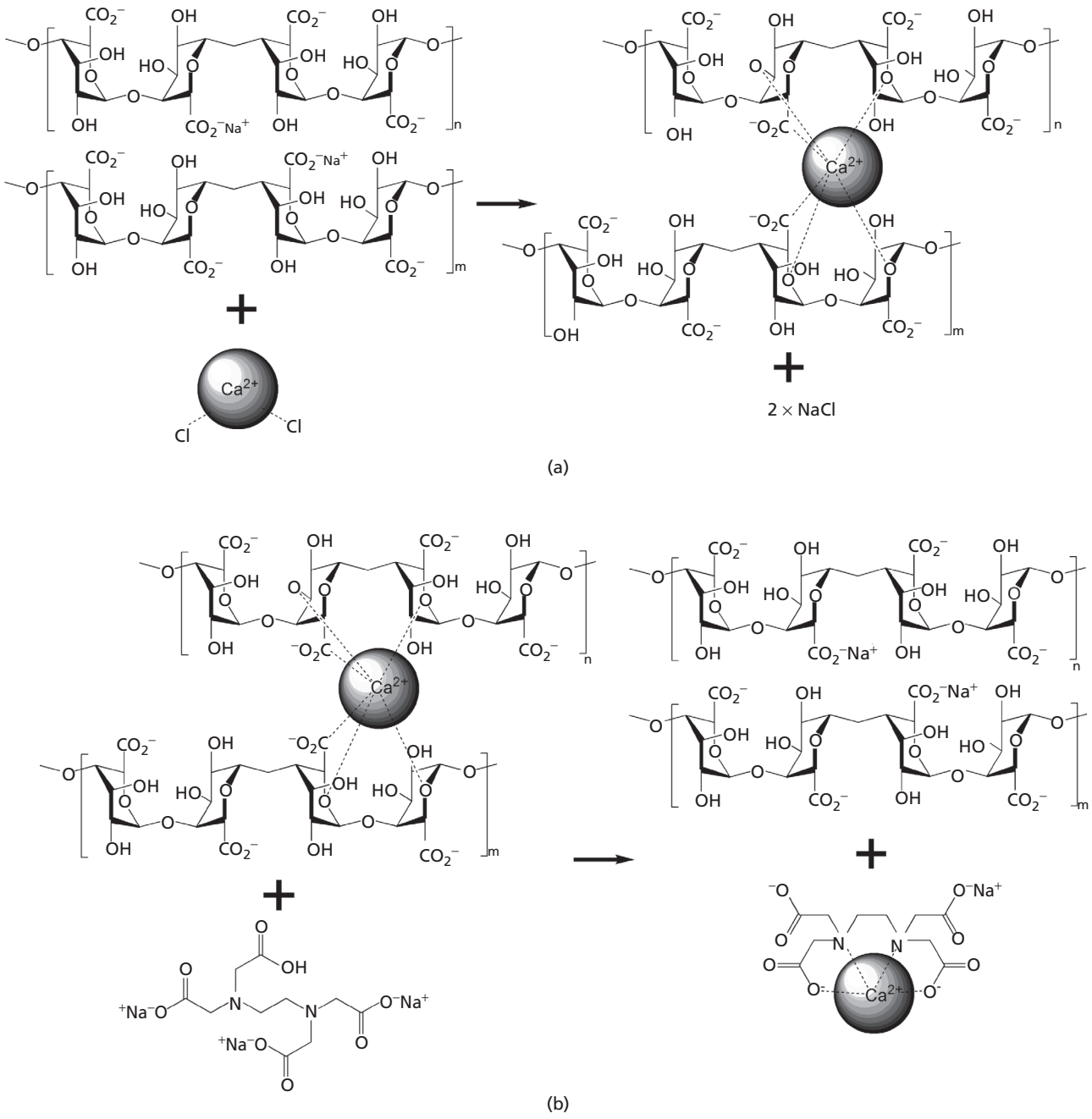

Figure 6. (a) Forming process of calcium alginate beads; (b) bead-dissolving processReprinted from Delaney *et al.*[87]

To interpret the experimental data obtained from indentation experiments, the above models are to be transformed into a force–displacement relationship, rather than in a strain-energy form. Lin *et al.*[92,106] extended the hyperelastic models into spherical indentation and provided the analytical solutions of these hyperelastic models. The transformation analogy was first proposed by Tabor[107,108] in the following forms:

$$2.\qquad \sigma^{*} = \frac{F}{\pi a^{2}}$$

$$3.\qquad \varepsilon^{*} = 0 \cdot 2\frac{a}{R}$$

where σ^{*} represents the indentation stress, ε^{*} represents the indentation strain, a represents the indentation contact radius and R

Hyperelastic models	Strain energy density functions	Uniaxial stress–stretch equations	References
Neo-Hookean	$W = C(I_1 - 3)$	$\sigma = 2C\left(\lambda - \lambda^{-2}\right)$	97
Mooney–Rivlin	$W = C_1(I_1 - 3) + C_2(I_2 - 3)$	$\sigma = 2C_1\left(\lambda - \lambda^{-2}\right) + 2C_2\left(1 - \lambda^{-3}\right)$	98
Fung	$W = \frac{C}{2b}\left\{\exp\left[b(I_1 - 3) - 1\right]\right\}$	$\sigma = C\left(\lambda - \lambda^{-2}\right)\exp\left[b(I_1 - 3)\right]$	99
Ogden	$W = \sum_{i=1}^{N} \frac{2C_i}{\alpha_i^2}\left(\lambda_x^{\alpha_i} + \lambda_y^{\alpha_i} + \lambda_z^{\alpha_i} - 3\right)$	$\sigma = \sum_{i=1}^{N} \frac{2C_i}{\alpha_i}\left(\lambda^{\alpha_i - 1} - \lambda^{-\alpha_i/2 - 1}\right)$	100
Yeoh	$W = \sum_{i=1}^{3} C_i (I_1 - 3)^i$	$\sigma = 2\left(\lambda^2 - \frac{1}{\lambda}\right)\sum_{i=1}^{3} iC_i (I_1 - 3)^{i-1}$	101

I_1 and I_2 represent the strain invariants; λ represents the stretch; C, C_1, C_2, b, C_i and α_i represent the fitting parameters.

Table 3. Hyperelastic models

represents the radius of indenter. The approach of Lin *et al.* is valid when the ratio of indentation depth to indenter radius (h/R) is smaller than 0·2.[92] However, when performing an atomic force microscopy-based indentation, the tip radius is usually so small that a low ratio of indentation depth to indenter radius may preclude the measurement accuracy. Zhang *et al.*[109] overcame this limitation by extending the ratio from 0·2 to 1 with dimensional analysis and finite-element method. Their work included the Neo-Hookean, Mooney–Rivlin, Fung and Arruda–Boyce models. In their approach, the force–displacement relationship was given in the following form:

$$4. \qquad P = G_0\sqrt{Rh}h\Pi\left(C, \frac{h}{R}\right)$$

where G_0 represents the initial shear modulus, R represents the radius of indenter, h represents the indentation depth, Π represents a dimensionless function and C represents a parameter of different model. By applying the finite-element method, the coefficients of Π for h/R varying from 0·01 to 1 were all obtained. In this manner, the force–displacement relationship was expressed in an explicit form and the range of h/R was extended to 1.

3.3 Viscoelastic models

As soft polymeric materials, hydrogels exhibit viscoelasticity, which is induced by the change in molecular conformation and the sliding between polymer chains. The common method to describe viscoelasticity is to combine springs and dashpots in various sequences and determine the parameters by fitting the experimental data. The most widely adopted models include the Maxwell, Viogt, Zernar, four-element, general Maxwell models and so on. Equation 5 provides an empirical Prony series to represent the general form of these models.

$$5. \qquad G(t) = G_\infty + \sum_{i=1}^{N} G_i \exp\left(\frac{-t}{\tau_i}\right)$$

In Equation 5, G represents the shear modulus, G_∞ represents the long-term modulus, N represents the number of Maxwell models in parallel, G_i represents the shear modulus of each Maxwell model, t represents time and τ_i represents the relaxation time in different orders. Because the hydrogels are usually regarded as incompressible, the Young's modulus, E, is just three times of shear modulus G. Hence, it is not listed it out in this article.

Roberts *et al.*[110] performed relaxation tests to compare the viscoelasticity of agarose and PEG hydrogels. A Prony series was applied to interpret the experimental data. The fitted parameter $G_\infty / G(0)$ was adopted as an indicator of the level of the stress relaxation. The comparison indicated that the agarose hydrogel displayed larger stress relaxation than the PEG hydrogel. A dynamic mechanical analysis (DMA) test was also performed in their work, and the results demonstrated that the storage modulus of agarose was more correlated to frequency. They suggested that the phenomena were due to the different cross-linking mechanisms of the two hydrogels. The agarose was cross-linked physically and the PEG was cross-linked covalently. The physical cross-linking is easier to slip, which explained the larger stress relaxation and higher dependency of storage modulus on frequency of agarose.

Small-scale indentation experiments are popular to characterise the viscoelasticity of hydrogels because they do not have a strict request upon the shape of the sample. For the spherical indenter, the load–displacement equation could be expressed by combining the Hertzian contact model and Boltzmann hereditary integrals.[111–113]

$$6. \qquad P(t) = \frac{8\sqrt{R}}{3}\int_0^t \overline{G}(t - \tau)\left[\frac{\mathrm{d}}{\mathrm{d}\tau}h^{3/2}(\tau)\right]\mathrm{d}\tau$$

where P represents the load, h represents the displacement, R represents the radius of the indenter and $\overline{G}(t)$ represents the

normalised shear modulus, which could once again be expressed by the Prony series as follows:

$$\overline{G}(t) = \overline{G_\infty} + \sum_{i=1}^{N} \overline{G_i} \exp\left(\frac{-t}{\tau_i}\right) \quad (7)$$

$$\overline{G_\infty} + \sum_{i=1}^{N} \overline{G_i} = 1 \quad (8)$$

Shapiro and Oyen[114] applied Equation 6 to characterise the viscoelasticity of poly(ethylene glycol) dimethacrylate (PEGDMA)/alginate hydrogel composite, single-component PEGDMA hydrogel and single-component alginate. The model fitted the experimental data well and provided indication to the viscoelasticity effectively.

Although the models discussed in this section described viscoelasticity successfully, they were less successful in interpreting the physical processes and polymer structures of hydrogels.[115]

3.4 Poroelastic models

The time-dependent elasticity of hydrogels is not only contributed by the viscosity of polymer chains, but also induced by the migration of viscous fluids inside the hydrogels, known as poroelasticity. The general concept of poroelasticity for hydrogels was first proposed by Biot[116] and developed by several research groups in the last decade.[117–120] The hydrogel is considered as a linear elastic polymer matrix drained by water, and the stress could be given by Equation 9.[121]

$$\sigma_{ij} = 2G\left[\varepsilon_{ij} + \varepsilon_{kk}\delta_{ij}\nu/(1-2\nu)\right] - \delta_{ij}(\mu-\mu_0)/\Omega \quad (9)$$

where G represents the shear modulus, ν represents the Poisson's ratio, μ represents the chemical potential of the solvent, Ω represents the volume per solvent molecule, which is constant, σ_{ij} represents the stress and ε_{ij} represents the strain. When fully swelled in solvent, the chemical potential of the solvent in hydrogel, μ, is equal to the chemical potential of the solvent in environment, μ_0. When the hydrogel deforms, the equilibrium is upset. Hence, a flux is driven by the chemical potential gradient according to Darcy's law, $J_i = -\left(k/\eta\Omega^2\right)\partial\mu/\partial x_i$, in pursuit of a new equilibrium state. In Darcy's law, J represents the flux, k represents the permeability and η represents the viscosity of the solvent. Besides, $\partial C/\partial t = -\partial J_k/\partial x_k$ according to the conservation of solvent molecules, where C represents the concentration of the solvent in gel, and $\varepsilon_{kk} = \Omega(C - C_0)$ according to the incompressible assumption of solvent molecules. Based on the equations above, the stress σ_{ij} is related to time t, so that the hydrogel exhibits a time-dependent behaviour. Besides, combining these equations together, the diffusion equation could be obtained as follows[121]:

$$\partial C/\partial t = D\nabla^2 C \quad (10)$$

where $D = \left[2(1-\nu)/(1-2\nu)\right]Gk/\eta$ represents the diffusivity.

Hu *et al.*[121] applied the poroelasticity theory into indentation relaxation tests on an alginate hydrogel. The indentation load $F(t)$ was given in the following form:

$$\frac{F(t) - F(\infty)}{F(0) - F(\infty)} = g\left(\frac{Dt}{a^2}\right) \quad (11)$$

where a represents the contact radius for different indenters. Equation 11 is in a quite simple form, which could be directly used to obtain poroelastic coefficients by fitting the experimental data. Cai *et al.*[122] from the same research group led by Zhigang Suo at Harvard University derived $F(t)$ by performing compressive relaxation tests on the same hydrogel. Although a little more complex to express, the result agreed well with that derived from the indentation tests. To study the poroelasticity under geometrical confine, Hu *et al.*[123] and Chan *et al.*[124] derived $F(t)$ of indentation relaxation on a thin gel layer, and indentation tests of different indentation depths were conducted on the PDMS gel in an organic solvent and PEG hydrogel in water, respectively. The poroelastic coefficients obtained from different indentation depths agreed with each other well, which validated their models.

The $\sqrt{Dt}$ has a dimension of length, which stands for the length of solvent migration over time t.[125] So the poroelastic relaxation time scale is related to the length scale of experiments.[119] In practice, it may take hours for an experiment with millimetre scale to fully relax,[119] which may lead to degradation of material. To shorten the time scale of relaxation, a possible method is to change the length scale of experiments. Kalcioglu *et al.*[119] performed contact experiments under both micro- and macro-size scales. Based on their results, the time scale was successfully shortened into seconds when the experimental length scale was in several micrometres and the poroelastic coefficients obtained from the microscopic experiments were in excellent agreement with those obtained from the macroscopic indentation tests.

In summary, compared to the viscoelasticity models that neglect the effects of solvent, poroelasticity models counts the time-dependent mechanical behaviour induced by the diffusion of the solvent in hydrogels. However, it is hard to find analytical solutions for the governing equations with complex loading, boundary and initial conditions. Therefore, computational methods are usually required to solve poroelastic problems.

3.5 Hybrid elastic models

The constitutive behaviour of hydrogels could be captured by hyperelasticity, viscoelasticity or poroelasticity models. However, they are either phenomenological or only consider part of the deformation mechanism. For instance, the Arruda–Boyce hyperelastic model considered the deformation of polymer chains but did not

include the time-dependent behaviour. Various viscoelastic models considered the time effect by counting the portion contributed by the polymer matrix but excluded the solvent's diffusion. Meanwhile, the poroelastic theory studied time dependence induced by the solvent inside the hydrogels but did not combine it with the viscosity of the polymer matrix. Hence, researchers were interested in combining or at least linking these models together in order to provide a comprehensive understanding on the constitutive behaviour of hydrogels, though only in elastic regime.

3.5.1 Visco-hyperelastic models

To combine viscoelasticity and poroelasticity together, Crichton *et al.*[126] provided a simple method. Although the studied object is skin instead of hydrogels, the methodology is universal. In their work, a two-term Prony series shown in Equation 13, which represents the viscoelasticity, was plugged into a single-term Ogden hyperelastic model (Equation 12) for contact problem with spherical indenter.

$$12.\quad P=\frac{40E_{\text{inst}}a^2}{9\alpha\left(1-\nu^2\right)}\left[\left(1-0\cdot2\frac{a}{R}\right)^{-\alpha/2-1}-\left(1-0\cdot2\frac{a}{R}\right)^{\alpha-1}\right]$$

$$13.\quad E_{\text{inst}}=E_{\text{r}}\left[1-g_1\left(1-e^{-\frac{t}{\tau_1}}\right)-g_2\left(1-e^{-\frac{t}{\tau_2}}\right)\right]$$

Another method to combine viscoelasticity and hyperelasticity together was proposed by Fung[99] and is known as quasi-linear viscoelasticity (QLV) theory. In Fung's approach, the viscoelastic part is represented by a normalised shear modulus, $\bar{G}(t)$, called reduced relaxation function. And the hyperelastic part could be represented as a function of stretch, $F^e(\lambda)$. By assuming that the hydrogel could be evaluated by the Boltzmann hereditary integrals, the load–stretch relationship under uniaxial tensile loading could be written as follows:

$$14.\quad F(\lambda,t)=\int_0^t \bar{G}(t-t')\frac{\mathrm{d}F^e(\lambda)}{\mathrm{d}\lambda}\frac{\mathrm{d}\lambda}{\mathrm{d}t'}\mathrm{d}t',$$

The function of stretch could be any hyperelastic models. $\bar{G}(t)$ could be written as a normalised Prony series, which is the same as Equations 7 and 8. Researchers[127–130] applied this method to evaluate the visco-hyperelasticity of not only hydrogels but also soft tissues by adopting various kinds of hyperelastic models under uniaxial loading directions for both monotonic, fatigue and load-relaxation experiments. Furthermore, after obtaining the coefficients of QLV model from one type of experiment, the QLV model could predict the force response of the experiment with another loading condition.[127,128]

Although the visco-hyperelastic models could not only fit the experimental data well even under complex loading conditions, but also predict the response in another loading scheme after the coefficients are obtained in one experiment, none of them counts for the migration of solvent.

3.5.2 Visco-poroelastic models

Both viscoelasticity and poroelasticity consider the time-dependent behaviour but on different aspects. Viscoelasticity is based on the change of molecular conformation and the sliding between polymer chains. Hence the relaxation time constant τ is independent of the length scale of the tested sample and contact area of indentation.[125,131] Unlike viscoelasticity, poroelasticity is characterised by the effective diffusivity D of the solvent in the network and depends on the type of the material and length scale of the material and experiment.[119] This difference could be used to decouple viscoelasticity and poroelasticity within a time-dependent framework.

As stated in the previous section, $\sqrt{D\tau}$ represents the length of solvent migration within a time comparable to viscoelastic relaxation time constant τ.[125] In an experiment with a time scale t and a length scale L, the comparison of t with τ and L^2/D could interpret whether the viscoelastic and poroelastic relaxations are completed or started, respectively, as summarised in Figure 7.[125] For example, if $t \gg \tau$ and $t \sim L^2/D$, the viscoelastic relaxation is already finished but poroelastic relaxation could be observed.

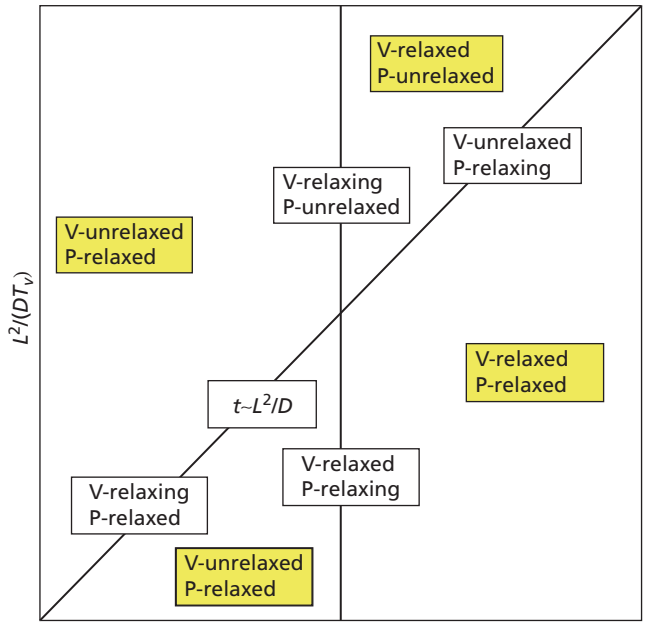

Figure 7. The verticle line $t \sim \tau_A$ and diagonal $t \sim L^2/D$ represent the viscoelasticity and poroelasticity under relaxing, respectively. These two lines separate the plane into four parts where each part represents a relaxation condition of the material. V represents viscoelasticity and P represents poroelasticityReprinted from Hu and Suo[125]

When $t \ll \tau$ and $t \ll L^2 / D$, both the viscoelastic and poroelastic relaxations have just started.

Hu *et al.*[132] and Strange *et al.*[133] studied the viscoelasticity and poroelasticity simultaneously by adjusting the indentation contact radius, which is one of the methods to change the length scale of the experiment. The viscoelastic and poroelastic parameters as well as elastic constants were obtained by comparing the stress-relaxation curves of different indentation contact radius with the theoretical models they derived. Wang *et al.*[118] separated the viscoelasticity and poroelasticity of the polyacrylamide–alginate IPN hydrogel apart by controlling the sample size and the length scale of the experiment. The two types of relaxation occurred one after the other. The finite-element calculation was performed to validate their method.

The combination of viscoelasticity and poroelasticity could describe the time-dependent constitutive behaviour of hydrogels well in simple loading conditions. But it is difficult to be executed under complex loading conditions due to the complexity in implementing the poroelastic theory.

4. Conclusions

In this review, the methods to tune the mechanical properties of hydrogels were briefly summarised. First, the mechanical properties were tuned based on the demands of versatile applications of hydrogels. Generally speaking, since most hydrogels are fragile and hard to handle, numerous efforts were devoted to fabricate tough hydrogels. However, hydrogels with higher porosity and lower modulus are also in favour for certain applications. Second, although it is the mechanical properties to be tuned, the effort is an interdisciplinary one, which involves physical, chemical, biological and many other science and engineering areas. Third, although due to the complexity of the structure of hydrogels, every tuning method may bring unexpected effects that are deviated from the original plan, optimisation can still be achieved by a smart design, which balances the structural properties and functionalities.

The constitutive models in elastic regime were reviewed in this article. Some of them are originate from other fields, such as models to predict the Young's modulus based on filler contents; some of them are phenomenological descriptions of observed behaviours, such as invariant-based and stretch-based hyperelastic models; and some of them are intrinsic models that provide mechanistic and physical principles, such as the Arruda–Boyce model. They all contributed in interpreting the experimental results and providing guidance to the mechanical tuning of hydrogels. However, because of the complexity of the hydrogel system, a universal model and/or framework that could capture and predict the comprehensive mechanical behaviour of hydrogels is still in hunt by the scientists and engineers. To achieve this goal, not only the macroscopic behaviours of hydrogels but also the detailed structure and the basic deformation mechanism should be considered.

Acknowledgements

The authors acknowledge the financial support from the City University of Hong Kong for Start-up Grant for New Faculty 7200274, Strategic Research Grant 2011SRG067 and Equipment Fund 9610217.

REFERENCES

1. Hoffman, A. S. Hydrogels for biomedical applications. *Advanced Drug Delivery Reviews* **2012**, *64*, 18–23.
2. Kirschner, C. M.; Anseth, K. S. Hydrogels in healthcare: from static to dynamic material microenvironments. *Acta Materialia* **2013**, *61*, 931–944.
3. Gupta, P.; Vermani, K.; Garg, S. Hydrogels: from controlled release to pH-responsive drug delivery. *Drug Discovery Today* **2002**, *7*, 569–579.
4. Hoare, T. R.; Kohane, D. S. Hydrogels in drug delivery: progress and challenges. *Polymer* **2008**, *49*, 1993–2007.
5. Qiu, Y.; Park, K. Environment-sensitive hydrogels for drug delivery. *Advanced Drug Delivery Reviews* **2001**, *53*, 321–339.
6. Omidian, H.; Park, K. Introduction to hydrogels. In *Biomedical Applications of Hydrogels Handbook* (Ottenbrite, R. M.; Park, K.; Okano, T. (eds.)). New York, NY: Springer, 2010, 1–16.
7. Sannino, A.; Demitri, C.; Madaghiele, M. Biodegradable cellulose-based hydrogels: design and applications. *Materials* **2009**, *2*, 353–373.
8. Hyon, S. H.; Cha, W. I.; Ikada, Y., *et al*. Poly(vinyl alcohol) hydrogels as soft contact lens material. *Journal of Biomaterials Science. Polymer Edition* **1994**, *5*, 397–406.
9. Tighe, B. J. A decade of silicone hydrogel development: surface properties, mechanical properties, and ocular compatibility. *Eye & Contact Lens* **2013**, *39*, 4–12.
10. Wichterle, O.; Lim, D. Hydrophilic gels for biological use. *Nature* **1960**, *185*, 117–118.
11. Drury, J. L.; Mooney, D. J. Hydrogels for tissue engineering: scaffold design variables and applications. *Biomaterials* **2003**, *24*, 4337–4351.
12. Hollister, S. J. Porous scaffold design for tissue engineering. *Nature Materials* **2005**, *4*, 518–524.
13. Lee, K. Y.; Mooney, D. J. Hydrogels for tissue engineering. *Chemical Reviews* **2001**, *101*, 1869–1879.
14. Billiet, T.; Vandenhaute, M.; Schelfhout, J.; Van Vlierberghe, S.; Dubruel, P. A review of trends and limitations in hydrogel-rapid prototyping for tissue engineering. *Biomaterials* **2012**, *33*, 6020–6041.
15. Huang, W.-C.; Chen, S.-Y.; Liu, D.-M. An amphiphilic silicone-modified polysaccharide molecular hybrid with in situ forming of hierarchical superporous architecture upon swelling. *Soft Matter* **2012**, *8*, 10868–10876.

16. Sudheesh Kumar, P. T.; Lakshmanan, V.-K.; Anilkumar, T. V., *et al*. Flexible and microporous chitosan hydrogel/nano ZnO composite bandages for wound dressing: in vitro and in vivo evaluation. *ACS Applied Materials & Interfaces* **2012**, *4*, 2618–2629.
17. Engler, A. J.; Sen, S.; Sweeney, H. L.; Discher, D. E. Matrix elasticity directs stem cell lineage specification. *Cell* **2006**, *126*, 677–689.
18. Awad, H. A.; Wickham, M. Q.; Leddy, H. A.; Gimble, J. M.; Guilak, F. Chondrogenic differentiation of adipose-derived adult stem cells in agarose, alginate, and gelatin scaffolds. *Biomaterials* **2004**, *25*, 3211–3222.
19. Erickson, I. E.; Huang, A. H.; Sengupta, S., *et al*. Macromer density influences mesenchymal stem cell chondrogenesis and maturation in photocrosslinked hyaluronic acid hydrogels. *Osteoarthritis and Cartilage* **2009**, *17*, 1639–1648.
20. Gilbert, P. M.; Havenstrite, K. L.; Magnusson, K. E., *et al*. Substrate elasticity regulates skeletal muscle stem cell self-renewal in culture. *Science* **2010**, *329*, 1078–1081.
21. Guilak, F.; Cohen, D. M.; Estes, B. T., *et al*. Control of stem cell fate by physical interactions with the extracellular matrix. *Cell Stem Cell* **2009**, *5*, 17–26.
22. Reilly, G. C.; Engler, A. J. Intrinsic extracellular matrix properties regulate stem cell differentiation. *Journal of Biomechanics* **2010**, *43*, 55–62.
23. Anseth, K. S.; Bowman, C. N.; Brannon-Peppas, L. Mechanical properties of hydrogels and their experimental determination. *Biomaterials* **1996**, *17*, 1647–1657.
24. Gaharwar, A. K.; Rivera, C. P.; Wu, C.-J.; Schmidt, G. Transparent, elastomeric and tough hydrogels from poly(ethylene glycol) and silicate nanoparticles. *Acta Biomaterialia* **2011**, *7*, 4139–4148.
25. Wu, C. J.; Wilker, J. J.; Schmidt, G. Robust and adhesive hydrogels from cross-linked poly(ethylene glycol) and silicate for biomedical use. *Macromolecular Bioscience* **2013**, *13*, 59–66.
26. Parlato, M.; Reichert, S.; Barney, N.; Murphy, W. L. Poly(ethylene glycol) hydrogels with adaptable mechanical and degradation properties for use in biomedical applications. *Macromolecular Bioscience* **2014**, *14*, 687–698.
27. Calvert, P. Hydrogels for soft machines. *Advanced Materials* **2009**, *21*, 743–756.
28. Gong, J. P. Why are double network hydrogels so tough? *Soft Matter* **2010**, *6*, 2583–2590.
29. Gong, J. P.; Katsuyama, Y.; Kurokawa, T.; Osada, Y. Double-network hydrogels with extremely high mechanical strength. *Advanced Materials* **2003**, *15*, 1155–1158.
30. Haque, Md. A.; Kurokawa, T.; Gong, J. P. Super tough double network hydrogels and their application as biomaterials. *Polymer* **2012**, *53*, 1805–1822.
31. Johnson, J. A.; Turro, N. J.; Koberstein, J. T.; Mark, J. E. Some hydrogels having novel molecular structures. *Progress in Polymer Science* **2010**, *35*, 332–337.
32. Peak, C. W.; Wilker, J. J.; Schmidt, G. A review on tough and sticky hydrogels. *Colloid and Polymer Science* **2013**, *291*, 2031–2047.
33. Weng, L.; Gouldstone, A.; Wu, Y.; Chen, W. Mechanically strong double network photocrosslinked hydrogels from *N,N*-dimethylacrylamide and glycidyl methacrylated hyaluronan. *Biomaterials* **2008**, *29*, 2153–2163.
34. Djonlagić, J.; Petrović, Z. S. Semi-interpenetrating polymer networks composed of poly(*N*-isopropyl acrylamide) and polyacrylamide hydrogels. *Journal of Polymer Science Part B: Polymer Physics* **2004**, *42*, 3987–3999.
35. Santin, M.; Huang, S. J.; Iannace, S., *et al*. Synthesis and characterization of a new interpenetrated poly(2-hydroxyethylmethacrylate)–gelatin composite polymer. *Biomaterials* **1996**, *17*, 1459–1467.
36. Stachowiak, A. N.; Bershteyn, A.; Tzatzalos, E.; Irvine, D. J. Bioactive hydrogels with an ordered cellular structure combine interconnected macroporosity and robust mechanical properties. *Advanced Materials* **2005**, *17*, 399–403.
37. Kurokawa, T.; Furukawa, H.; Wang, W.; Tanaka, Y.; Gong, J. P. Formation of a strong hydrogel–porous solid interface via the double-network principle. *Acta Biomaterialia* **2010**, *6*, 1353–1359.
38. Nemir, S.; Hayenga, H. N.; West, J. L. PEGDA hydrogels with patterned elasticity: novel tools for the study of cell response to substrate rigidity. *Biotechnology and Bioengineering* **2010**, *105*, 636–644.
39. Seliktar, D. Designing cell-compatible hydrogels for biomedical applications. *Science* **2012**, *336*, 1124–1128.
40. Henderson, K. J.; Zhou, T. C.; Otim, K. J.; Shull, K. R. Ionically cross-linked triblock copolymer hydrogels with high strength. *Macromolecules* **2010**, *43*, 6193–6201.
41. Sun, J.-Y.; Zhao, X.; Illeperuma, W. R., *et al*. Highly stretchable and tough hydrogels. *Nature* **2012**, *489*, 133–136.
42. Tuncaboylu, D. C.; Sari, M.; Oppermann, W.; Okay, O. Tough and self-healing hydrogels formed via hydrophobic interactions. *Macromolecules* **2011**, *44*, 4997–5005.
43. Gaharwar, A. K.; Rivera, C.; Wu, C. J.; Chan, B. K.; Schmidt, G. Photocrosslinked nanocomposite hydrogels from PEG and silica nanospheres: structural, mechanical and cell adhesion characteristics. *Materials Science and Engineering: C* **2013**, *33*, 1800–1807.
44. Lin, W.-C.; Marcellan, A.; Hourdet, D.; Creton, C. Effect of polymer–particle interaction on the fracture toughness of silica filled hydrogels. *Soft Matter* **2011**, *7*, 6578–6582.
45. Pasqui, D.; Atrei, A.; Giani, G.; De Cagna, M.; Barbucci, R. Metal oxide nanoparticles as cross-linkers in polymeric hybrid hydrogels. *Materials Letters* **2011**, *65*, 392–395.
46. Wang, Q.; Hou, R.; Cheng, Y.; Fu, J. Super-tough double-network hydrogels reinforced by covalently compositing with silica-nanoparticles. *Soft Matter* **2012**, *8*, 6048–6056.
47. Yun, J.; Im, J. S.; Oh, A., *et al*. pH-sensitive photocatalytic activities of TiO_2/poly(vinyl alcohol)/poly(acrylic acid)

composite hydrogels. *Materials Science and Engineering: B* **2011**, *176*, 276–281.
48. Andrade, Â. L.; Fabris, J. D.; Ardisson, J. D.; Valente, M. A.; Ferreira, J. M. F. Effect of tetramethylammonium hydroxide on nucleation, surface modification and growth of magnetic nanoparticles. *Journal of Nanomaterials* **2012**, *2012*, 15.
49. El-Mohdy, H. L. A. Radiation synthesis of nanosilver/poly vinyl alcohol/cellulose acetate/gelatin hydrogels for wound dressing. *Journal of Polymer Research* **2013**, *20*, 1–12.
50. Wei, Q.-B.; Fu, F.; Zhang, Y.-Q.; Tang, L. Preparation, characterization, and antibacterial properties of pH-responsive P(MMA-co-MAA)/silver nanocomposite hydrogels. *Journal of Polymer Research* **2014**, *21*, 1–9.
51. Choi, Y.; Simonsen, J. Cellulose nanocrystal-filled carboxymethyl cellulose nanocomposites. *Journal of Nanoscience and Nanotechnology* **2006**, *6*, 633–639.
52. Kim, B.; Hong, D.; Chang, W. V. Swelling and mechanical properties of pH-sensitive hydrogel filled with polystyrene nanoparticles. *Journal of Applied Polymer Science* **2013**, *130*, 3574–3587.
53. Di Giacomo, R.; Maresca, B.; Angelillo, M., *et al*. Bio-nano-composite materials constructed with single cells and carbon nanotubes: mechanical, electrical and optical properties. *IEEE Transactions on Nanotechnology* **2013**, *12*, 1026–1030.
54. Liu, J.; Cui, L.; Kong, N.; Barrow, C. J.; Yang, W. RAFT controlled synthesis of graphene/polymer hydrogel with enhanced mechanical property for pH-controlled drug release. *European Polymer Journal* **2014**, *50*, 9–17.
55. Mandal, S. K.; Kar, T.; Das, P. K. Pristine carbon-nanotube-included supramolecular hydrogels with tunable viscoelastic properties. *Chemistry – European Journal* **2013**, *19*, 12486–12496.
56. Shin, S. R.; Bae, H.; Cha, J. M., *et al*. Carbon nanotube reinforced hybrid microgels as scaffold materials for cell encapsulation. *ACS Nano* **2012**, *6*, 362–372.
57. Xu, Y.; Lin, Z.; Huang, X., *et al*. Flexible solid-state supercapacitors based on three-dimensional graphene hydrogel films. *ACS Nano* **2013**, *7*, 4042–4049.
58. Lin, W.-C.; Fan, W.; Marcellan, A.; Hourdet, D.; Creton, C. Large strain and fracture properties of poly(dimethylacrylamide)/silica hybrid hydrogels. *Macromolecules* **2010**, *43*, 2554–2563.
59. Douce, J.; Boilot, J.-P.; Biteau, J.; Scodellaro, L.; Jimenez, A. Effect of filler size and surface condition of nano-sized silica particles in polysiloxane coatings. *Thin Solid Films* **2004**, *466*, 114–122.
60. Ji, X. L.; Jing, J. K.; Jiang, W.; Jiang, B. Z. Tensile modulus of polymer nanocomposites. *Polymer Engineering & Science* **2002**, *42*, 983–993.
61. Mishra, S.; Sonawane, S. H.; Singh, R. P. Studies on characterization of nano $CaCO_3$ prepared by the in situ deposition technique and its application in PP-nano $CaCO_3$ composites. *Journal of Polymer Science Part B: Polymer Physics* **2005**, *43*, 107–113.
62. Radford, K. C. The mechanical properties of an epoxy resin with a second phase dispersion. *Journal of Materials Science* **1971**, *6*, 1286–1291.
63. Kinloch, A. J.; Maxwell, D. L.; Young, R. J. The fracture of hybrid-particulate composites. *Journal of Materials Science* **1985**, *20*, 4169–4184.
64. Maxwell, D.; Young, R. J.; Kinloch, A. J. Hybrid particulate-filled epoxy-polymers. *Journal of Materials Science Letters* **1984**, *3*, 9–12.
65. Ou, Y.; Yang, F.; Yu, Z.-Z. A new conception on the toughness of nylon 6/silica nanocomposite prepared via in situ polymerization. *Journal of Polymer Science Part B: Polymer Physics* **1998**, *36*, 789–795.
66. Wu, C.-J.; Gaharwar, A. K.; Chan, B. K.; Schmidt, G. Mechanically tough pluronic F127/laponite nanocomposite hydrogels from covalently and physically cross-linked networks. *Macromolecules* **2011**, *44*, 8215–8224.
67. Friedrich, K.; Fakirov, S.; Zhang, Z. *Polymer composites: from nano- to macro-scale*. New York, NY: Springer, 2005.
68. Counto, U. J. The effect of the elastic modulus of the aggregate on the elastic modulus, creep and creep recovery of concrete. *Magazine of Concrete Research* **1964**, *16*, 129–138.
69. Einstein, A. Über die von der molekularkinetischen Theorie der Wärme geforderte Bewegung von in ruhenden Flüssigkeiten suspendierten Teilchen. *Annalen der Physik* **1905**, *322*, 549–560.
70. Einstein, A. *Investigations on the Theory of the Brownian Movement*. New York, NY: Courier Dover Publications, 1956.
71. Fu, S.-Y.; Xu, G.; Mai, Y.-W. On the elastic modulus of hybrid particle/short-fiber/polymer composites. *Composites Part B: Engineering* **2002**, *33*, 291–299.
72. Guth, E. Theory of filler reinforcement. *Journal of Applied Physics* **1945**, *16*, 20–25.
73. Lewis, T. B.; Nielsen, L. E. Dynamic mechanical properties of particulate-filled composites. *Journal of Applied Polymer Science* **1970**, *14*, 1449–1471.
74. Mooney, M. The viscosity of a concentrated suspension of spherical particles. *Journal of Colloid Science* **1951**, *6*, 162–170.
75. Nielsen, L. E. Generalized equation for the elastic moduli of composite materials. *Journal of Applied Physics* **1970**, *41*, 4626–4627.
76. Nielsen, L. E. Dynamic mechanical properties of polymers filled with agglomerated particles. *Journal of Polymer Science: Polymer Physics Edition* **1979**, *17*, 1897–1901.
77. Verbeek, C. J. R. The influence of interfacial adhesion, particle size and size distribution on the predicted mechanical properties of particulate thermoplastic composites. *Materials Letters* **2003**, *57*, 1919–1924.

78. Guvendiren, M.; Burdick, J. A. Engineering synthetic hydrogel microenvironments to instruct stem cells. *Current Opinion in Biotechnology* **2013**, *24*, 841–846.
79. Cui, J.; Lackey, M. A.; Madkour, A. E., *et al*. Synthetically simple, highly resilient hydrogels. *Biomacromolecules* **2012**, *13*, 584–588.
80. Cui, J.; Lackey, M. A.; Tew, G. N.; Crosby, A. J. Mechanical properties of end-linked PEG/PDMS hydrogels. *Macromolecules* **2012**, *45*, 6104–6110.
81. Liu, T. Y.; Chen, S. Y.; Lin, Y. L.; Liu, D. M. Synthesis and characterization of amphiphatic carboxymethyl-hexanoyl chitosan hydrogel: water-retention ability and drug encapsulation. *Langmuir* **2006**, *22*, 9740–9745.
82. Huang, W.-C.; Liu, K.-H.; Liu, T.-C.; Liu, D.-M.; Chen, S.-Y. Synergistic hierarchical silicone-modified polysaccharide hybrid as a soft scaffold to control cell adhesion and proliferation. *Acta Biomaterialia* **2014**, *10*, 3546–3556.
83. Bignon, A.; Chouteau, J.; Chevalier, J., *et al*. Effect of micro- and macroporosity of bone substitutes on their mechanical properties and cellular response. *Journal of Materials Science: Materials in Medicine* **2003**, *14*, 1089–1097.
84. Cordell, J. M.; Vogl, M. L.; Wagoner Johnson, A. J. The influence of micropore size on the mechanical properties of bulk hydroxyapatite and hydroxyapatite scaffolds. *Journal of Mechanical Behavior of Biomedical Materials* **2009**, *2*, 560–570.
85. Sopyan, I.; Mel, M.; Ramesh, S.; Khalid, K. A. Porous hydroxyapatite for artificial bone applications. *Science and Technology of Advanced Materials* **2007**, *8*, 116–123.
86. Huang, G. Y.; Zhou, L. H.; Zhang, Q. C., *et al*. Microfluidic hydrogels for tissue engineering. *Biofabrication* **2011**, *3*, 012001.
87. Delaney, J. T.; Liberski, A. R.; Perelaer, J.; Schubert, U. S. Reactive inkjet printing of calcium alginate hydrogel porogens – a new strategy to open-pore structured matrices with controlled geometry. *Soft Matter* **2010**, *6*, 866–869.
88. Lévesque, S. G.; Lim, R. M.; Shoichet, M. S. Macroporous interconnected dextran scaffolds of controlled porosity for tissue-engineering applications. *Biomaterials* **2005**, *26*, 7436–7446.
89. Tokuyama, H.; Kanehara, A. Novel synthesis of macroporous poly (*N*-isopropylacrylamide) hydrogels using oil-in-water emulsions. *Langmuir* **2007**, *23*, 11246–11251.
90. Lu, G. D.; Yan, Q. Z.; Ge, C. C. Preparation of porous polyacrylamide hydrogels by frontal polymerization. *Polymer International* **2007**, *56*, 1016–1020.
91. Chan, B. K.; Wippich, C. C.; Wu, C. J.; Sivasankar, P. M.; Schmidt, G. Robust and semi-interpenetrating hydrogels from poly(ethylene glycol) and collagen for elastomeric tissue scaffolds. *Macromolecular Bioscience* **2012**, *12*, 1490–1501.
92. Lin, D. C.; Shreiber, D. I.; Dimitriadis, E. K.; Horkay, F. Spherical indentation of soft matter beyond the Hertzian regime: numerical and experimental validation of hyperelastic models. *Biomechanics and Modeling in Mechanobiology* **2009**, *8*, 345–358.
93. Sneddon, I. N. The relation between load and penetration in the axisymmetric boussinesq problem for a punch of arbitrary profile. *International Journal of Engineering Science* **1965**, *3*, 47–57.
94. Derjaguin, B. V.; Muller, V. M.; Toporov, Yu. P. Effect of contact deformations on the adhesion of particles. *Journal of Colloid and Interface Science* **1975**, *53*, 314–326.
95. Johnson, K. L.; Kendall, K.; Roberts, A. D. Surface energy and the contact of elastic solids. *Proceedings of Royal Society of London Series A: Mathematical and Physical Sciences* **1971**, *324*, 301–313.
96. Chyasnavichyus, M.; Young, S. L.; Tsukruk, V. V. Probing of polymer surfaces in the viscoelastic regime. *Langmuir* **2014**, *30*, 10566–10582.
97. Rivlin, R. S. Large elastic deformations of isotropic materials. IV. Further developments of the general theory. *Philosophical Transactions of Royal Society of London Series A: Mathematical and Physical Sciences* **1948**, *241*, 379–397.
98. Mooney, M. A theory of large elastic deformation. *Journal of Applied Physics* **1940**, *11*, 582–592.
99. Fung, Y. C. Elasticity of soft tissues in simple elongation. *American Journal of Physiology* **1967**, *213*, 1532–1544.
100. Ogden, R. W. Large deformation isotropic elasticity – on the correlation of theory and experiment for incompressible rubberlike solids. *Proceedings of Royal Society of London Series A: Mathematical and Physical Sciences* **1972**, *326*, 565–584.
101. Yeoh, O. H. Some forms of the strain energy function for rubber. *Rubber Chemistry and Technology* **1993**, *66*, 754–771.
102. Arruda, E. M.; Boyce, M. C. A three-dimensional constitutive model for the large stretch behavior of rubber elastic materials. *Journal of Mechanics and Physics of Solids* **1993**, *41*, 389–412.
103. Sasson, A.; Patchornik, S.; Eliasy, R.; Robinson, D.; Haj-Ali, R. Hyperelastic mechanical behavior of chitosan hydrogels for nucleus pulposus replacement – experimental testing and constitutive modeling. *Journal of Mechanical Behavior of Biomedical Materials* **2012**, *8*, 143–153.
104. Faghihi, S.; Karimi, A.; Jamadi, M.; Imani, R.; Salarian, R. Graphene oxide/poly(acrylic acid)/gelatin nanocomposite hydrogel: experimental and numerical validation of hyperelastic model. *Materials Science and Engineering: C* **2014**, *38*, 299–305.
105. Zhao, X. A theory for large deformation and damage of interpenetrating polymer networks. *Journal of Mechanics and Physics of Solids* **2012**, *60*, 319–332.
106. Lin, D. C.; Dimitriadis, E. K.; Horkay, F. Robust strategies for automated AFM force curve analysis – I. Non-adhesive indentation of soft, inhomogeneous materials. *Journal of Biomechanical Engineering* **2007**, *129*, 430–440.
107. Tabor, D. A simple theory of static and dynamic hardness. *Proceedings of Royal Society of London Series A: Mathematical and Physical Sciences* **1948**, *192*, 247–274.

108. Tabor, D. *The Hardness of Metals*. Oxford, UK: Clarendon Press, 1951.
109. Zhang, M. G.; Cao, Y. P.; Li, G. Y.; Feng, X. Q. Spherical indentation method for determining the constitutive parameters of hyperelastic soft materials. *Biomechanics and Modeling in Mechanobiology* **2014**, *13*, 1–11.
110. Roberts, J. J.; Earnshaw, A.; Ferguson, V. L.; Bryant, S. J. Comparative study of the viscoelastic mechanical behavior of agarose and poly(ethylene glycol) hydrogels. *Journal of Biomedical Materials Research Part B: Applied Biomaterials* **2011**, *99*, 158–169.
111. Sakai, M. Time-dependent viscoelastic relation between load and penetration for an axisymmetric indenter. *Philosophical Magazine A* **2002**, *82*, 1841–1849.
112. Oyen, M. L. Analytical techniques for indentation of viscoelastic materials. *Philosophical Magazine* **2006**, *86*, 5625–5641.
113. Mattice, J. M.; Lau, A. G.; Oyen, M. L.; Kent, R. W. Spherical indentation load-relaxation of soft biological tissues. *Journal of Materials Research* **2006**, *21*, 2003–2010.
114. Shapiro, J. M.; Oyen, M. L. Viscoelastic analysis of single-component and composite PEG and alginate hydrogels. *Acta Mechanica Sinica* **2014**, *30*, 7–14.
115. Oyen, M. L. Mechanical characterisation of hydrogel materials. *International Materials Reviews* **2014**, *59*, 44–59.
116. Biot, M. A. General theory of three-dimensional consolidation. *Journal of Applied Physics* **1941**, *12*, 155–164.
117. Wang, X.; Hong, W. A visco-poroelastic theory for polymeric gels. *Proceedings of Royal Society A: Mathematical, Physical and Engineering Sciences* **2012**, *468*, 3824–3841.
118. Wang, Q.-M.; Mohan, A. C.; Oyen, M. L.; Zhao, X.-H. Separating viscoelasticity and poroelasticity of gels with different length and time scales. *Acta Mechanica Sinica* **2014**, *30*, 20–27.
119. Kalcioglu, Z. I.; Mahmoodian, R.; Hu, Y.; Suo, Z.; Van Vliet, K. J. From macro- to microscale poroelastic characterization of polymeric hydrogels via indentation. *Soft Matter* **2012**, *8*, 3393–3398.
120. Hong, W.; Zhao, X.; Zhou, J.; Suo, Z. A theory of coupled diffusion and large deformation in polymeric gels. *Journal of Mechanics and Physics of Solids* **2008**, *56*, 1779–1793.
121. Hu, Y.; Zhao, X.; Vlassak, J. J.; Suo, Z. Using indentation to characterize the poroelasticity of gels. *Applied Physics Letters* **2010**, *96*, 121904.
122. Cai, S.; Hu, Y.; Zhao, X.; Suo, Z. Poroelasticity of a covalently crosslinked alginate hydrogel under compression. *Journal of Applied Physics* **2010**, *108*, 113514.
123. Hu, Y.; Chan, E. P.; Vlassak, J. J.; Suo, Z. Poroelastic relaxation indentation of thin layers of gels. *Journal of Applied Physics* **2011**, *110*, 086103.
124. Chan, E. P.; Hu, Y.; Johnson, P. M.; Suo, Z.; Stafford, C. M. Spherical indentation testing of poroelastic relaxations in thin hydrogel layers. *Soft Matter* **2012**, *8*, 1492–1498.
125. Hu, Y.; Suo, Z. Viscoelasticity and poroelasticity in elastomeric gels. *Acta Mechanica Solida Sinica* **2012**, *25*, 441–458.
126. Crichton, M. L.; Donose, B. C.; Chen, X., *et al*. The viscoelastic, hyperelastic and scale dependent behaviour of freshly excised individual skin layers. *Biomaterials* **2011**, *32*, 4670–4681.
127. Lucas, S. R.; Bass, C. R.; Crandall, J. R., *et al*. Viscoelastic and failure properties of spine ligament collagen fascicles. *Biomechanics and Modeling in Mechanobiology* **2009**, *8*, 487–498.
128. Lucas, S. R.; Bass, C. R.; Salzar, R. S., *et al*. Viscoelastic properties of the cervical spinal ligaments under fast strain-rate deformations. *Acta Biomaterialia* **2008**, *4*, 117–125.
129. Karimi, A.; Navidbakhsh, M. Measurement of the nonlinear mechanical properties of a poly(vinyl alcohol) sponge under longitudinal and circumferential loading. *Journal of Applied Polymer Science* **2014**, *131*, 40257
130. Karimi, A.; Navidbakhsh, M.; Beigzadeh, B. A visco-hyperelastic constitutive approach for modeling polyvinyl alcohol sponge. *Tissue & Cell* **2014**, *46*, 97–102.
131. Schapery, R. A. Nonlinear viscoelastic and viscoplastic constitutive equations based on thermodynamics. *Mechanics of Time-Dependent Materials* **1997**, *1*, 209–240.
132. Hu, Y.; Chen, X.; Whitesides, G. M.; Vlassak, J. J.; Suo, Z. Indentation of polydimethylsiloxane submerged in organic solvents. *Journal of Materials Research* **2011**, *26*, 785–795.
133. Strange, D. G. T.; Fletcher, T. L.; Tonsomboon, K., *et al*. Separating poroviscoelastic deformation mechanisms in hydrogels. *Applied Physics Letters* **2013**, *102*, 031913.